



## Particle size dependence of CO tolerance of anode PtRu catalysts for polymer electrolyte fuel cells

Toshiro Yamanaka\*, Tatsuya Takeguchi\*\*, Guoxiong Wang, Ernee Noryana Muhamad, Wataru Ueda

Catalysis Research Center, Hokkaido University, Kita-21 Nishi-10, Kita-ku, Sapporo 001-0021, Japan

### ARTICLE INFO

#### Article history:

Received 6 January 2010

Received in revised form 1 March 2010

Accepted 3 April 2010

Available online 10 April 2010

#### Keywords:

Polymer electrolyte fuel cell

Catalyst

PtRu

CO tolerance

### ABSTRACT

An anode catalyst for a polymer electrolyte fuel cell must be CO-tolerant, that is, it must have the function of hydrogen oxidation in the presence of CO, because hydrogen fuel gas generated by the steam reforming process of natural gas contains a small amount of CO. In the present study, PtRu/C catalysts were prepared with control of the degree of Pt–Ru alloying and the size of PtRu particles. This control has become possible by a new method of heat treatment at the final step in the preparation of catalysts. The CO tolerances of PtRu/C catalysts with the same degree of Pt–Ru alloying and with different average sizes of PtRu particles were thus compared. Polarization curves were obtained with pure H<sub>2</sub> and CO/H<sub>2</sub> (CO concentrations of 500–2040 ppm). It was found that the CO tolerance of highly dispersed PtRu/C (high dispersion (HD)) with small PtRu particles was much higher than that of poorly dispersed PtRu/C (low dispersion (LD)) with large metal particles. The CO tolerance of PtRu/C (HD) was higher than that of any commercial PtRu/C. The high CO tolerance of PtRu/C (HD) is thought to be due to efficient concerted functions of Pt, Ru, and their alloy.

© 2010 Elsevier B.V. All rights reserved.

### 1. Introduction

Much interest has recently been shown in polymer electrolyte fuel cells (PEFCs) as highly efficient energy conversion systems. Hydrogen gas is usually used as a fuel gas to operate PEFCs. Since H<sub>2</sub> gas is usually generated by a steam reforming process of natural gas, the resultant H<sub>2</sub> gas contains a small amount of CO. This CO deactivates catalysts at the anode of a PEFC, and development of an anode catalyst with high CO tolerance is therefore required for practical use of PEFCs [1,2]. Among previously reported catalysts, platinum–ruthenium alloy is well known to have the highest CO tolerance [3]. However, it cannot accept H<sub>2</sub> fuel gas with CO higher than 100 ppm. Various studies have been carried out to increase CO tolerance of PtRu by improving methods for preparing PtRu and by modification of PtRu with another metal or metal oxides [4–9].

A bifunctional mechanism, reduction of CO sticking probability and modification of the electronic structure, is thought to be involved in the mechanism of CO tolerance. In the bifunctional mechanism [10–14], H<sub>2</sub>O that is supplied to humidify the metal electrode assembly (MEA) is converted to OH<sup>−</sup> and H<sub>2</sub> on the Ru surface and then OH<sup>−</sup> reacts with CO that is adsorbed on the Pt

surface, resulting in the formation of CO<sub>2</sub> and thus elimination of CO on the Pt surface. In the second mechanism, sticking probability of CO on Pt is reduced by Ru. In the third mechanism, the electronic structure of Pt is modified by Ru, leading to improved catalytic functions.

To enhance CO tolerance of PtRu catalysts, it is necessary to control the structure of PtRu. It has been reported that high CO tolerance was achieved when Ru was deposited on a highly dispersed Pt/C catalyst with subsequent annealing to induce alloying between Pt and Ru [15]. This alloying is an important factor for achieving high CO tolerance. However, the alloying process at a high temperature also leads to coalescence of PtRu particles, resulting in the formation of large PtRu particles [16–18], and it has therefore been difficult to control the degree of alloying and the degree of dispersion independently. Preparation of highly alloyed and highly dispersed PtRu/C catalysts has been particularly difficult. Information on the effects of particle size on CO tolerance is still lacking. Separate control of the degree of alloying and the degree of dispersion (particle sizes) is needed to obtain such information.

In this work, we made PtRu/C anode catalysts with almost independent control of the degree of Pt–Ru alloying and PtRu particle sizes. In our method for preparing catalysts, the degree of Pt–Ru alloying could be kept constant and sufficiently high, while the sizes of PtRu particles were changed. It is possible to make catalysts that consist of small PtRu particles with high degrees of alloying. This control is performed in the final heating step of catalyst preparation in H<sub>2</sub> and involves only changing the period for elevation of temper-

\* Corresponding author. Tel.: +81 11 706 9119; fax: +81 11 706 9163.

\*\* Corresponding author. Tel.: +81 11 706 9165; fax: +81 11 706 9163.

E-mail addresses: [yama@cat.hokudai.ac.jp](mailto:yama@cat.hokudai.ac.jp) (T. Yamanaka), [takeguch@cat.hokudai.ac.jp](mailto:takeguch@cat.hokudai.ac.jp) (T. Takeguchi).

ature and maximum temperature in extremely wide ranges with no change in other procedures for preparation of catalysts. Thus, it has become possible to compare CO tolerance of catalysts with the same high degree of alloying and different average particle sizes that are made by basically the same method. CO tolerance of PtRu/C with small PtRu particles was found to be much higher than that of PtRu/C with large PtRu particles and also higher than that of any commercial PtRu/C catalysts. The correlation between sizes of metal particles and CO tolerance is discussed.

## 2. Experimental

### 2.1. Preparation of PtRu/C

In the present study, PtRu/C catalysts of Pt:Ru = 2:3 and Pt:Ru = 1:3 were prepared. These PtRu/C catalysts were prepared by deposition of Ru onto a commercial Pt/C catalyst with 40 wt% Pt as follows. This method is similar to that reported previously [15]. First, 1.25 g of Pt/C, 1 or 2 g of  $\text{RuCl}_3 \cdot n\text{H}_2\text{O}$ , 25 mL of alcohol and 200 mL of distilled water were mixed and stirred in a glass bottle at a high temperature. During this process, Ru was reduced by methanol and stuck to Pt/C. The molar ratios of Pt:Ru in the catalysts and  $\text{RuCl}_3 \cdot n\text{H}_2\text{O}$  were 2:3 or 1:3. After 12 h of stirring, the catalysts obtained were filtered and washed with hot distilled water. Then the catalysts were dried in air at 80 °C overnight.

Next, catalysts were reduced in  $\text{H}_2/\text{Ar}$  (5%  $\text{H}_2$ ) at high temperatures with a new method. In this reduction, the temperature of the catalyst was monotonously elevated in an oven from room temperature to a maximum temperature ( $T_{\text{max}}$ ).  $T_{\text{max}}$  was widely changed from 25 °C (i.e., no heating) to 900 °C. The period ( $P$ ) for elevating the temperature from room temperature to  $T_{\text{max}}$  was widely changed from 10 to 500 min. The oven was turned off immediately when the temperature reached  $T_{\text{max}}$  to rapidly cool the catalyst. When  $T_{\text{max}}$  was 900 °C, the temperature decreased from 900 to 500 °C in 18 min and decreased from 500 °C to room temperature in about 50 min. The time that it took to cool the catalyst from  $T_{\text{max}}$  to room temperature was shorter when  $T_{\text{max}}$  was lower than 900 °C. The resultant sizes of PtRu particles (degree of dispersion) and the degree of Pt–Ru alloying could be controlled simply by changing  $P$  and  $T_{\text{max}}$ . It was found that  $P$  and  $T_{\text{max}}$  were good parameters to control degrees of dispersion and alloying, respectively. Thus, a PtRu/C catalyst with high dispersion (HD) and a PtRu/C catalyst with low dispersion (LD) with well-alloyed PtRu were prepared. The conditions of these heating processes, especially extremely short heating at high temperature, are quite different from those of heating in previously reported works.

### 2.2. Structural evaluation

XRD patterns of PtRu/C catalysts were obtained by using a powder X-ray diffractometer (RIGAKU, RINT 2000). The tube current used for Cu  $K\alpha$  radiation was 40 mA and the tube voltage was 40 kV. Silicon powder (Standard Reference Material 640C, NIST) was used as a reference sample to correct the angle shift of the powder X-ray diffractometer. The angular region of the  $2\theta$  scan was set between 10° and 85°, and the scan rate was 1°  $\text{min}^{-1}$ . The peak profile of the (220) reflection of Pt fcc structure was fitted with a Gaussian function. The degree of alloying and the particle sizes were evaluated from the position and width of the optimum Gaussian functions. Catalyst morphology was also investigated by using a Hitachi HD-2000 scanning electron microscope (SEM) and a scanning transmission electron microscope (STEM) instrument with an electron energy of 200 kV and a beam current of 30  $\mu\text{A}$ .

### 2.3. Preparation of an MEA (membrane electrode assembly)

A P50T carbon paper provided by Ballard Material Products Inc. was used as the backing layer of the anode and cathode. Carbon black ink was made by mixing Vulcan XC-72 carbon black and polytetrafluoroethylene (PTFE, Aldrich). The ink was painted onto the backing layer to form a microporous layer. The amount of carbon black painted was about 1.2  $\text{mg cm}^{-2}$  and the PTFE content in the microporous layer was 40 wt%.

To make the anode catalyst layer on the microporous layer, PtRu/C catalysts and Nafion solution were ultrasonically suspended in water and the resultant catalyst ink was painted onto the microporous layer at 70 °C. The loading of Pt in the anode catalyst layer was 0.5  $\text{mg cm}^{-2}$  and the Nafion content was 10 wt%. Then a Nafion solution was brushed onto the surface of the anode catalyst layer with a dry ionomer loading of about 0.5  $\text{mg cm}^{-2}$ .

In all cases, an identical cathode catalyst layer was prepared by the same procedure as that described above. A commercial Pt/C catalyst (40 wt% Pt) was painted instead of PtRu/C catalysts, and the loadings of Pt and Nafion in the resultant cathode layer were the same as those in the anode catalyst layer. Finally, the anode and cathode (22 mm  $\times$  22 mm) were placed onto the two sides of a Nafion NRE-212 membrane (Aldrich) and hot-pressed at 135 °C and 4 MPa for 10 min to form the MEA.

### 2.4. Single cell test

The MEA was assembled into a single cell with flow field plates made of graphite and copper end plates attached to a heater (FC05-01SP, ElectroChem, Inc.) [19]. The single cell was connected to fuel cell test equipment (Kofloc Corp.) consisting of mass flow-rate controllers, temperature controllers and humidifiers for the reactant gases. Pure  $\text{H}_2$  (or  $\text{H}_2/\text{CO}$  mixture) and oxygen were supplied at a flow rate of 80  $\text{mL min}^{-1}$  to the anode and cathode at ambient pressure, respectively. During the measurement, a single cell was operated at 75 °C, and the anode and cathode humidifiers were set at 75 and 70 °C, respectively. The current was scanned from 0 A with a rate of 0.02  $\text{A cm}^{-2} \text{ s}^{-1}$  and the scan was stopped when the cell voltage became smaller than 0.3 V. The scan was repeated for 2 h with an interval of 5 min at each concentration of CO in order to stabilize the concentration of CO.

### 2.5. CO stripping voltammetry

CO stripping voltammetry measurements were carried out in a 250 mL three-electrode cell (HR200, Hokuto Denko Corp.) at room temperature. A commercial glassy carbon (GC) electrode (HR2-D1-GC-5, 5 mm in diameter, 0.196  $\text{cm}^2$ , Hokuto Denko Corp.), a Pt-wire electrode (Hokuto Denko Corp.) and a saturated calomel electrode (SCE, Hokuto Denko Corp.) were used as a working electrode, a counter electrode and a reference electrode, respectively. The potential of the working electrode was controlled by an Iviumstat Electrochemical Interface System (Ivium Technologies B.V.). Six milligram of the catalyst was dispersed in a mixture of 2 mL water, 3 mL ethanol and 50  $\mu\text{L}$  Nafion solution (5 wt%, Aldrich) with ultrasonic stirring to form a homogeneous ink. The catalyst layer was prepared by dropping 10  $\mu\text{L}$  of the ink onto a GC disk electrode by a microsyringe and drying at room temperature. All potential values in this paper are referred to a reversible hydrogen electrode (RHE). For CO stripping voltammetry, pure CO was supplied into the electrolyte solution (0.1 M  $\text{HClO}_4$ ) for 20 min at a fixed potential of 0.05 V and then high-purity (99.99%) Ar was bubbled for 30 min to remove the CO dissolved in the electrolyte solution. The current–potential cycles were obtained from 0.05 to 1.2 V at a scan rate of 10  $\text{mV s}^{-1}$ . The calculated peak charge  $Q_{\text{CO}}$  was used to compare the electrochemical surface area of the catalysts,

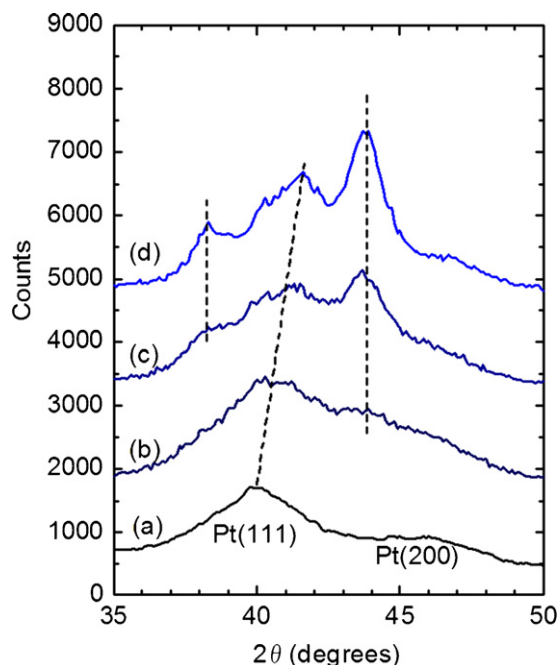


**Fig. 1.** XRD patterns obtained for four PtRu/C (Pt:Ru = 1:3) catalysts reduced at different temperatures in a short period,  $P = 10$  min. Values of  $T_{\max}$  were (a) 25 °C, (b) 250 °C, (c) 450 °C and (d) 900 °C.

which was obtained with the assumption of a monolayer of linearly adsorbed CO and charge density required for electro-oxidation of 0.42 mC cm<sup>-2</sup>.

### 3. Results and discussion

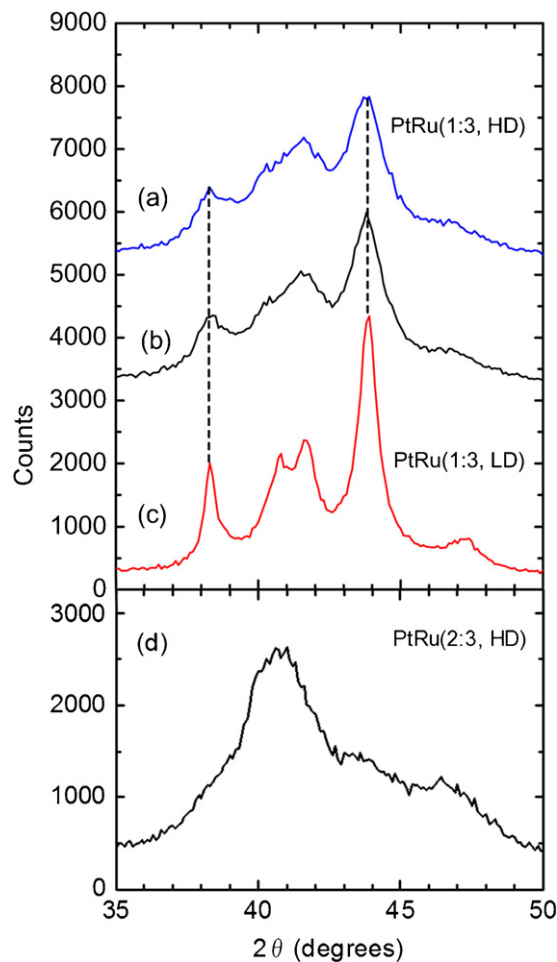
Fig. 1a–d shows XRD patterns obtained for four PtRu/C (Pt:Ru = 1:3) catalysts reduced in H<sub>2</sub> with different values of  $T_{\max}$  for extremely short time ( $P = 10$  min). Values of  $T_{\max}$  were (a) 25 °C (i.e., without heating), (b) 250 °C, (c) 450 °C and (d) 900 °C. In (a) there are two peaks at 40° and 47°, which are very close to the angles of diffractions from (1 1 1) and (2 0 0) planes of platinum. This XRD pattern is very similar to that of a Pt/C catalyst without deposition of Ru. This indicates that platinum and ruthenium were not alloyed. No diffractions from ruthenium were observed, and the degree of crystallization of ruthenium was very low.

With increases in  $T_{\max}$ , the peak of diffraction from the (1 1 1) plane shifted to higher angles and additional peaks appeared as shown by b–d. The additional peaks also shifted to higher angles. These results indicate that the lattice constants changed due to alloying between platinum and ruthenium as  $T_{\max}$  was increased. The sizes of particles were estimated from the width of the peak of X-ray diffraction from the (2 2 0) plane. With increases in  $T_{\max}$ , the average sizes of particles increased from 2.3 to 5.0 nm. While increase in size during the alloying process could not be completely avoided, the increase in size was minimized by using a very short period of annealing. The XRD pattern shown in Fig. 1d indicates a high degree of alloying even though the average particle size was as small as 5 nm, indicating a highly dispersed and highly alloyed catalyst.

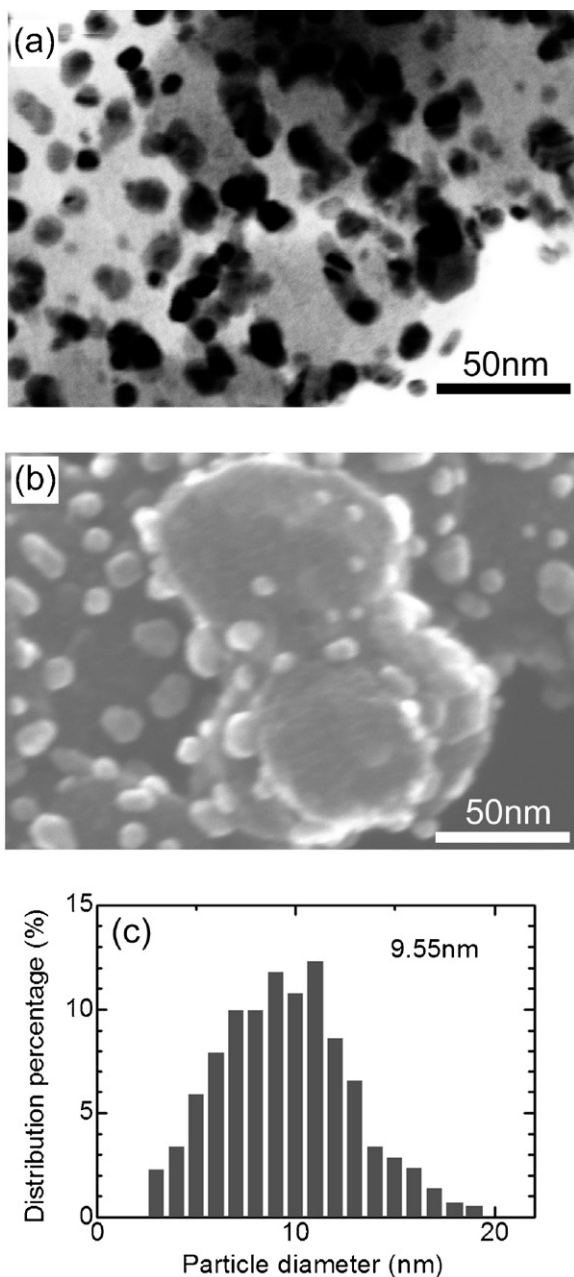
Fig. 2a–c shows XRD patterns obtained for three PtRu/C (Pt:Ru = 1:3) catalysts reduced with a constant  $T_{\max}$  of 900 °C and different values of  $P$ . The values of  $P$  were (a) 10 min, (b) 30 min and (c) 500 min. All XRD patterns show peaks at the same angles, indicating that platinum and ruthenium in all catalysts were well alloyed. However, the widths of peaks increased with decreasing  $P$ , indicating that the average particle size decreased. This indicates

that it is possible to prepare highly dispersed catalysts by decreasing the period of annealing while maintaining a sufficiently high degree of alloying of Pt–Ru. This technique is very fundamental and important because an alloying process usually leads to coalescence of metal particles, resulting in the formation of large particles, and it is generally difficult to prepare small particles with a high degree of alloying. The average sizes estimated from the position and width of the peak due to diffraction from the (2 2 0) plane were 5.0 nm (a), 5.7 nm (b) and 13.2 nm (c). The catalysts with XRD patterns shown in Fig. 2a and c are referred to as PtRu/C (1:3, high dispersion (HD)) and PtRu/C (1:3, low dispersion (LD)), respectively. PtRu/C (2:3, HD) was also prepared by the same method as that used for PtRu/C (1:3, HD) with change in the molar ratio of Pt to Ru. The average sizes of metal particles of PtRu/C (2:3, HD) estimated from the position and width of the peak due to diffraction from the (2 2 0) plane at 69.0° were 3.1 nm, which is smaller than the value of 5.0 nm for PtRu/C (1:3, HD).

Fig. 3a and b shows STEM and SEM images of PtRu/C (1:3, LD), respectively. The scale bars indicate 50 nm. Since the atomic numbers of metals are larger than that of carbon, metal particles are shown by dark particles in the STEM image and by bright particles in the SEM image. These images show relatively large particles of PtRu. The distribution of sizes of particles was obtained from measurements of sizes of about 200 particles in these images, as shown in Fig. 3c. The sizes ranged from 3 to 20 nm, and the average particle size was calculated to be 9.6 nm.



**Fig. 2.** XRD patterns obtained for three PtRu/C (Pt:Ru = 1:3) catalysts reduced with  $T_{\max} = 900$  °C for different periods  $P$ . Values of  $P$  were (a) 10 min, (b) 30 min and (c) 500 min. (d) shows an XRD pattern obtained for PtRu/C (2:3, HD) reduced with  $T_{\max} = 900$  °C and  $P = 10$  min.



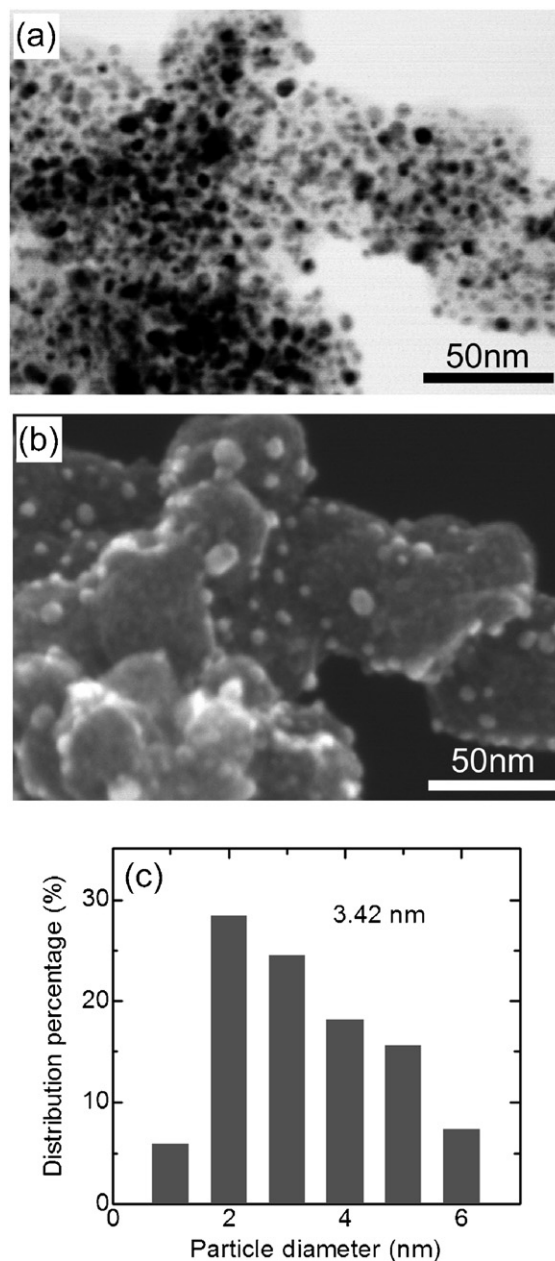
**Fig. 3.** STEM image (a) and SEM image (b) of PtRu/C (1:3, LD). Scale bars indicate 50 nm. (c) shows the distribution of particle sizes obtained from (a).

Fig. 4a and b shows STEM and SEM images of PtRu/C (1:3, HD), respectively. The scale bars indicate 50 nm. The particles are much smaller than those in the images in Fig. 3a and b, which is consistent with the large width of peaks in the XRD pattern shown in Fig. 2a. The distribution of sizes of particles derived from about 200 particles in these images is shown in Fig. 4c. The sizes were less than 6 nm, and the average particle size was calculated to be 3.4 nm.

Fig. 5a and b shows STEM and SEM images of PtRu/C (2:3, HD), respectively. The scale bars indicate 50 nm. The particles are further smaller than those in the images in Fig. 4a and b, which is consistent with the fact that the average size of PtRu/C (2:3, HD) estimated from the XRD pattern is smaller than that of PtRu/C (1:3, HD). The distribution of sizes of metal particles derived from about 200 particles in these images is shown in Fig. 5c. The average particle size was 2.35 nm.

Fig. 6a shows *I*–*V* curves for PtRu/C (1:3, HD) (thin solid line), PtRu/C (2:3, HD) (dashed line), PtRu/C (1:3, LD) (dotted line), and PtRu/C (2:3, commercial (CM)) (thick solid line) obtained with pure H<sub>2</sub>. The alloying degree of PtRu/C (2:3, CM) is similar to that of PtRu/C (2:3, HD) since the position of (2 2 0) XRD peak described on its data sheet was 69.00° which is almost the same as that (69.0°) of PtRu/C (2:3, HD). With increases in current, the cell voltages decreased. The PtRu/C (2:3, HD) catalyst showed the best performance, i.e., the highest cell voltages, though the performances of all catalysts were basically the same.

Fig. 6b shows *I*–*V* curves for PtRu/C (1:3, HD) (thin solid line), PtRu/C (2:3, HD) (dashed line), PtRu/C (1:3, LD) (dotted line), and PtRu/C (2:3, CM) (thick solid line) obtained with CO/H<sub>2</sub> (2040 ppm CO). The performances of all catalysts became worse, i.e., the cell voltages were lower than those obtained with pure H<sub>2</sub> shown in Fig. 6a. This is because the anode catalysts were deactivated by CO. The PtRu/C (2:3, HD) and PtRu/C (1:3, HD) catalysts still showed



**Fig. 4.** STEM image (a) and SEM image (b) of PtRu/C (1:3, HD). Scale bars indicate 50 nm. (c) shows the distribution of particle sizes obtained from (a).

**Table 1**  
Voltage and decrease in voltage by CO at current density of  $0.20 \text{ A cm}^{-2}$ .

	Average size of metal particles (nm)		Voltage and (voltage drop) (V)		
	XRD	STEM	Pure H <sub>2</sub>	500 ppm CO	2040 ppm CO
PtRu/C (1:3, LD)	13.2	9.55	0.764	0.627 (0.137)	0.418 (0.346)
PtRu/C (1:3, HD)	5.0	3.42	0.788	0.754 (0.034)	0.716 (0.072)
PtRu/C (2:3, HD)	3.1	2.35	0.783	0.751 (0.033)	0.705 (0.078)
PtRu/C (2:3, CM)	3.62 <sup>a</sup>		0.774	0.704 (0.070)	0.585 (0.189)

<sup>a</sup> The average particle size for PtRu/C (2:3, CM) was estimated from the values for full width at half maximum ( $2.66^\circ$ ) and position ( $69.00^\circ$ ) of 2 2 0 diffraction described in the data sheet of the commercial catalyst.

excellent performances, indicating high CO tolerance, compared with the performances of PtRu/C (2:3, CM) and PtRu/C (1:3, LD). The average particle size of PtRu/C (2:3, CM) was calculated to be 3.62 nm from the position ( $69.00^\circ$ ) and full width at half maximum ( $2.66^\circ$ ) of 2 2 0 X-ray diffraction which was described in the data

sheet of this catalyst. This average size was larger than the average size (3.1 nm) of PtRu/C (2:3, HD) derived from the position ( $68.92^\circ$ ) and width ( $3.13^\circ$ ) of 2 2 0 X-ray diffraction. The positions of 2 2 0 diffraction for PtRu/C (2:3, HD) and PtRu/C (2:3, CM) were close, indicating that the degrees of alloying of PtRu/C (2:3, HD) and PtRu/C (2:3, CM) were very similar. These results indicate that highly dispersed catalysts show high CO tolerance. The difference between voltages with CO/H<sub>2</sub> and with pure H<sub>2</sub> is an indicator of CO tolerance. Voltages and decreases in voltage by CO at the current density of  $0.24 \text{ A cm}^{-2}$  are summarized with average particle sizes in Table 1. It is clearly seen that catalysts with small particles show high CO tolerance for both Pt:Ru = 1:3 and 2:3. While alloying of Pt and Ru is well known to be an important factor for achieving high CO tolerance, the effect of dispersion on CO tolerance has not been reported.

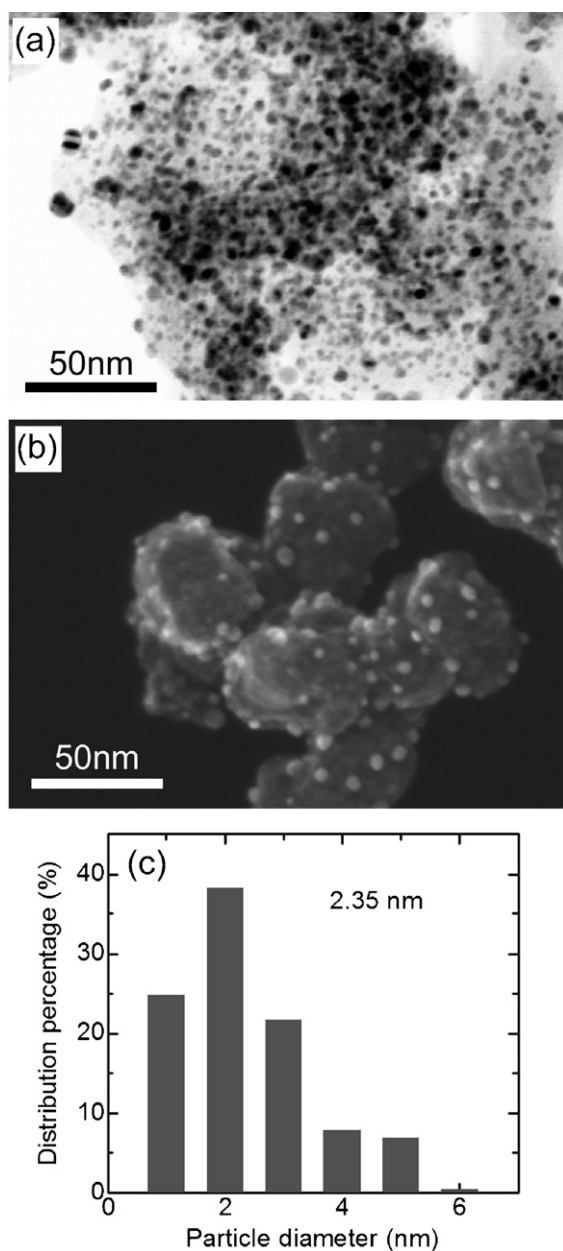


**Fig. 5.** STEM image (a) and SEM image (b) of PtRu/C (2:3, HD). (a) and (b) show images of different parts. Scale bars indicate 50 nm. (c) shows the distribution of particle sizes obtained from (a).

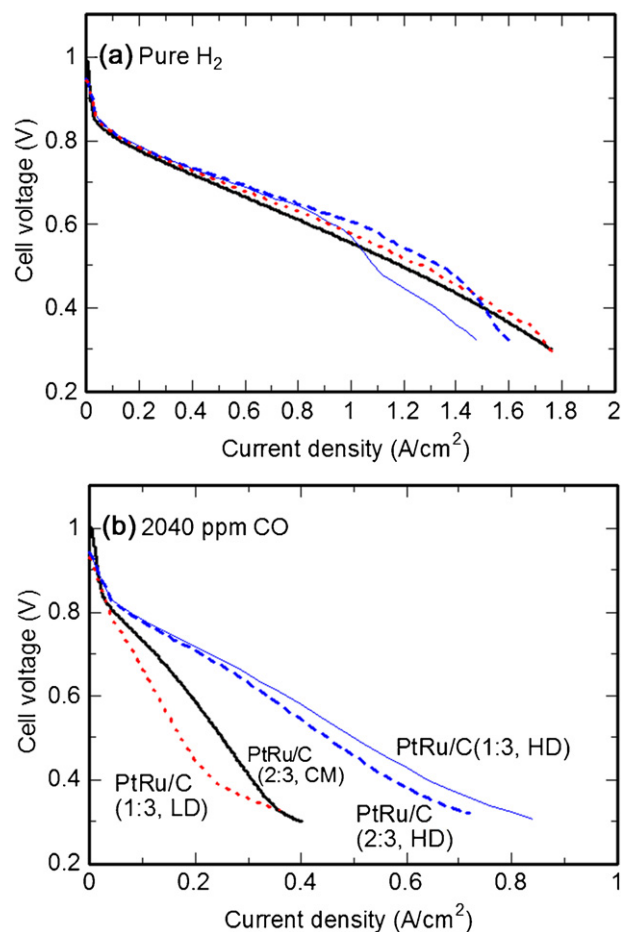


**Fig. 6.** (a) *I*-*V* curves for PtRu/C (1:3, HD) (thin solid line), PtRu/C (2:3, HD) (dashed line), PtRu/C (1:3, LD) (dotted line), and PtRu/C (2:3, CM) (thick solid line) obtained with pure H<sub>2</sub>. (b) *I*-*V* curves for PtRu/C (1:3, HD) (thin solid line), PtRu/C (2:3, HD) (dashed line), PtRu/C (1:3, LD) (dotted line), and PtRu/C (2:3, CM) (thick solid line) obtained with H<sub>2</sub>/CO (2040 ppm CO).

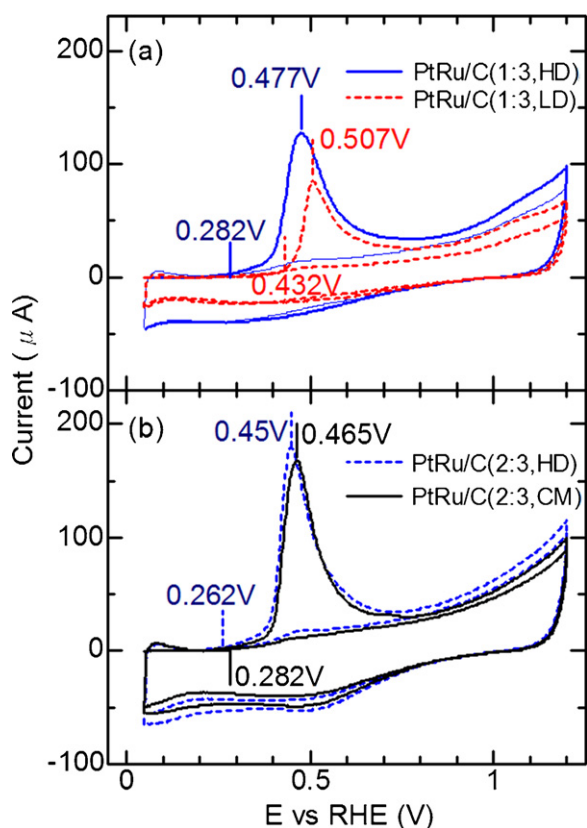


**Fig. 7.** CO stripping voltammetry. (a) PtRu/C (1:3, HD) and PtRu/C (1:3, LD). (b) PtRu/C (2:3, HD) and PtRu/C (2:3, CM).

The activity for CO electrochemical oxidation is often considered as an indicator of CO tolerance. Fig. 7a and b shows comparison of CO stripping voltammetry between PtRu/C (1:3, HD) and PtRu/C (1:3, LD), and PtRu/C (2:3, HD) and PtRu/C (2:3, CM), respectively. The electrochemical surface area of PtRu/C (1:3, HD) calculated from these results was  $47.0 \text{ m}^2 \text{ g}^{-1}$  (Pt + Ru), which was larger than that of PtRu/C (1:3, LD) ( $21.9 \text{ m}^2 \text{ g}^{-1}$  (Pt + Ru)). In addition, the onset and peak potentials for PtRu/C (1:3, HD) (0.28 V, 0.48 V) were lower than those for PtRu/C (1:3, LD) (0.43, 0.507 V). These different potential values cannot be explained as the effect of different surface areas. These results suggest that high CO tolerance of PtRu/C (1:3, HD) is due to the high efficiency for CO oxidation that is not due to the large surface area although the large surface area may also enhance CO tolerance in part. The electrochemical surface area of PtRu/C (2:3, HD) ( $62.8 \text{ m}^2 \text{ g}^{-1}$  (Pt + Ru)) was slightly larger than that of PtRu/C (2:3, CM) ( $59.0 \text{ m}^2 \text{ g}^{-1}$  (Pt + Ru)). The onset and peak potentials for PtRu/C (2:3, HD) (0.26, 0.45 V) were slightly lower than those for PtRu/C (2:3, CM) (0.28, 0.465 V). The difference in electrochemical surface areas, onset and peak potentials between PtRu/C (2:3, HD) and PtRu/C (2:3, CM) is small, but difference in CO tolerance between these two catalysts shown in Fig. 6 is significant. This suggests that CO tolerance is affected also by additional unknown structural factors (makers and preparation methods of the two catalysts are different) that are difficult to evaluate from electrochemical surface areas and activities of electrochemical CO oxidation.

The high CO tolerance of PtRu/C (1:3, HD) and PtRu/C (2:3, HD) is probably due to efficient concerted functions of Pt, Ru and their alloy. Pt has the function of  $\text{H}_2$  dissociation, yielding  $\text{H}^+$  that penetrates through Nafion to the cathode. When CO is adsorbed on Pt, this catalytic function is interrupted. On the other hand, Ru has the function to create  $\text{OH}^-$ . CO adsorbed on Pt is oxidized by

$\text{OH}^-$  provided by adjacent Ru [3]. Therefore, high CO tolerance is achieved if  $\text{OH}^-$  is efficiently supplied from Ru to Pt. These concerted functions operate efficiently on catalysts with a high degree of dispersion since Pt, Ru and their alloy all exist within the diffusion length of reactants. It is well known that high dispersion of catalysts is an important factor for achieving high catalytic activities. The results of this study indicate that dispersion of PtRu is also an important factor for achieving high CO tolerance of PtRu catalysts of PEFCs. The surface condition of carbon may affect gas diffusion and water transfer resistance in MEA. The final heat treatment in  $\text{H}_2$  in preparation of the three catalysts should result in reduction of carbon surfaces. It is not clear whether different heat treatments of these catalysts resulted in different surface conditions of carbon.

It has been reported that increase in the ratio of Ru to Pt enhances CO tolerance of PtRu/C [15]. In that work, the average particle sizes (4–5 nm for Pt:Ru = 1:1 and 6–8 nm for Pt:Ru = 1:2) were larger than those in the present study. In the present study, PtRu/C (1:3, HD) showed higher CO tolerance than that of PtRu/C (2:3, HD), but the difference was not significant.

#### 4. Conclusions

PtRu/C catalysts were prepared with control of both the degree of Pt–Ru alloying and the sizes of PtRu particles, which has so far been difficult. This control was achieved by a new method of heating in the final step of catalyst preparation in which the period for elevating the temperature and the maximum temperature of the catalyst were changed in extremely wide ranges, while other processes in making the catalyst were unchanged. It was found that  $P$  and  $T_{\text{max}}$  were good parameters to control degrees of dispersion and alloying, respectively. The CO tolerances of PtRu/C catalysts with the same degree of Pt–Ru alloying and with different average sizes of PtRu particles were thus compared, and the dependence of CO tolerance on particle size was investigated. The CO tolerance of highly dispersed PtRu/C (HD) with small PtRu particles was found to be much higher than that of poorly dispersed PtRu/C (LD) with large PtRu particles, indicating the importance of dispersion of PtRu to achieve high CO tolerance. The CO tolerance of PtRu/C (HD) was higher than that of any commercial PtRu/C catalysts. This high CO tolerance was achieved by extremely short annealing at high temperature. The high CO tolerance of PtRu/C (HD) is probably due to efficient concerted functions of Pt, Ru and their alloy. The method for controlling the degrees of alloying and dispersion would be applicable for the preparation of other alloy catalysts.

#### Acknowledgment

This study was supported by Strategic Development of PEFC Technologies for Practical Application Grant Program in 07003615-0 from New Energy and Industrial Technology Development Organization (NEDO) of Japan.

#### References

- [1] T.R. Ralph, M.P. Hogarth, *Platinum Met. Rev.* 46 (2002) 117.
- [2] J.J. Baschuk, X.G. Li, *Int. J. Energy. Res.* 25 (2001) 695.
- [3] M. Watanabe, S. Motoo, *J. Electroanal. Chem.* 60 (1975) 275.
- [4] E.N. Muhamad, T. Takeguchi, G. Wang, Y. Anzai, W. Ueda, *J. Electroanal. Chem.* 156 (2009) B32.
- [5] G. Wang, T. Takeguchi, Y. Zhang, E.N. Muhamad, M. Sadakane, S. Ye, W. Ueda, *J. Electroanal. Chem.* 156 (2009) B862.
- [6] European Patent 0838872 A2 (1998).
- [7] Y. Morimoto, E.B. Yeager, *J. Electroanal. Chem.* 441 (1998) 77.
- [8] T. Ioroi, Z. Shiroma, S. Yamazaki, N. Fujiwara, H. Senoh, K. Yasuda, *Proceedings of the 46th Battery Symposium in Japan, 2005*, p. 124 (in Japanese).
- [9] S.J. Cooper, A.G. Gunner, G. Hoogers, D. Thompssett, *Proceedings of 2nd International Symposium on "New Materials for Fuel Cell and Modern Battery System"*, 1997, p. 286.

- [10] H.A. Gasteiger, N. Markovic, P.N. Ross, E.J. Cairns, *J. Phys. Chem.* 98 (1994) 617.
- [11] H.A. Gasteiger, N.M. Markovic, P.N. Ross, *J. Phys. Chem.* 99 (1995) 8290.
- [12] K.A. Friedrich, K.P. Geysers, U. Linke, U. Stimming, J. Stumper, *J. Electroanal. Chem.* 402 (1996) 123.
- [13] H.F. Oetjen, V.M. Schmidt, U. Stimming, F. Trila, *J. Electrochem. Soc.* 143 (1996) 3838.
- [14] M. Iwase, S. Kawatsu, *Proc. Electrochem. Soc.* 95 (1995) 12.
- [15] T. Tada, Y. Yamamoto, S. Mitsushima, K. Ota, *Electrochemistry* 76 (2008) 813.
- [16] B. Yang, Q. Lu, Y. Wang, L. Zhuang, J. Lu, P. Liu, J. Wang, R. Wang, *Chem. Mater.* 15 (2003) 3552.
- [17] G.A. Camara, M.J. Giz, V.A. Paganin, E.A. Ticianelli, *J. Electroanal. Chem.* 537 (2002) 21.
- [18] M.-K. Min, J. Cho, K. Cho, H. Kim, *Electrochim. Acta* 45 (2000) 4211.
- [19] T. Takeguchi, Y. Anzai, R. Kikuchi, K. Eguchi, W. Ueda, *J. Electrochem. Soc.* 154 (2007) B1132.